Fireclay Refractories from Ugandan Kaolinitic Minerals

John Baptist Kirabira[1], Gunnar Wijk[2], Stefan Jonsson[3], Joseph Kadoma Byaruhanga[1]

[1] Department of Mechanical Engineering, Faculty of Technology, Makerere University, Kampala, Uganda. [2] Höganäs Bjuf AB, Bjuv, Sweden. [3] Materials Science and Engineering, Royal Institute of Technology, Stockholm, Sweden.

In the present work, two deposits, one of kaolin and the other of ball clay, located in Uganda were investigated for the possibility of manufacturing fireclay refractories. Kaolin from the Mutaka deposit was used as the main source of alumina while ball clay from Mukono was the main plasticizer and binder material. The formulated green body was consolidated by wet pressing and fired at 1350°C in a tunnel kiln. Characterization of the sintered articles was done by X-ray diffraction, scanning electron microscopy, and chemical composition (ICP-AES). In addition, technological properties related to thermal conductivity, thermal shock, alkali resistance, water absorption, porosity, shrinkage, permanent linear change, linear thermal expansion, refractoriness under load, and cold crushing strength were determined. The properties of the articles manufactured from these naturally occurring raw minerals reveal that they compare favorably with those of parallel types. Thus, the raw materials can be exploited for industrial production.

Keywords: fireclay refractory, kaolin, clay.

Introduction

The technical goals of manufacture of a given refractory are embodied in its properties and performance in the intended application. Fireclay bricks are normally made of fired clay that is selected, ground, mixed with water, formed in presses, dried and then fired at temperatures in excess of 1300°C. The fireclay brick is the most common refractory brick in high temperature applications and is used for structural linings of furnaces, boilers, incinerators, domestic fireplaces, coke ovens, cement kilns, foundries and gas furnaces among other high temperature confining wall structures. The chemical composition of a fireclay brick is typically 60-80% silica, 25-45% alumina, 1-2.5% iron oxide, 0.5-1.5% calcia, 0.5-0.7 magnesia and 1-2% of potash and soda [2-4]. The indicated variations are due to differences in the compositions of the clays used, which will depend not only on the source of raw materials but also the selected beneficiation. The mechanical properties of a fireclay brick are mainly determined by the amount of mullite formed during firing. Naturally this is determined by the chemical composition of clays used in production.

The insights of manufacturing a brick have to do with the final phase composition which is determined by the chemical composition of the raw materials. According to previous work by Kirabira et al. [5] and Nyakairu et al. [6], Uganda is considered well endowed with quality ceramic raw materials, which can be used for manufacture of refractories. The current consumption and need is being filled by importation of refractories from Europe, India, SE Asia and South Africa. Consequently, the present work aims to develop fireclay refractory bricks from naturally occurring raw materials from Uganda. Similar product development studies have been done elsewhere [7-12].

The two materials used in this work were kaolin from Mutaka and clay from Mukono. Kaolin is used as the main source of alumina and ball clay as the binder material. A product mix was formulated and industrial samples were produced at Höganäs Bjuf AB, Sweden. Thermal, mechanical, chemical and physical tests have been carried out in conformance with international standards. A detailed description about the processing and evaluation of the ultimate article properties is given.

Materials and Methods

Raw materials and manufacture of industrial bricks. The raw materials, Mutaka kaolin and Mukono ball clay were previously characterized by Kirabira et al, [13] and the results from the chemical analysis are reproduced in **Table 1**. A uniform batch mix of approximately 1000 kg were prepared by milling a mixture of 70% Mutaka kaolin and 30% Mukono ball clay in a ball mill for 8h. The ball mill was emptied and the mixture left to dry into a stiff mud. The stiff mud was formed into bricks using hand moulds, dried and pre-calcined at 1350°C for 4h before being left to cool in the furnace. After cooling the calcined material, grog, was crushed and graded into three different sizes; course (1-3mm), middle (0.25-1mm) and fine (< 0.25mm) using standard sieves.

A mixture of 30% course, 20% middle and 30% fine of the graded grog was mixed with 20% milled kaolin/clay binder of the same composition. Accordingly, the resultant mixture was wetted to about 15% moisture, kneaded, extruded and formed at about 400 MPa, using a hydraulic

Table 1. Chemical composition of raw materials and final brick in comparison with commercial types.

Oxide	Raw Materials		Final Brick	Commercial types
	Kaolin [wt %]	Ball clay [wt %]	[wt %]	[wt %]
SiO_2	48.800	67.200	64.700	65-69 [25]
Al_2O_3	36.000	18.200	30.600	25-45 [25]
Fe_2O_3	0.238	2.830	0.880	1.5-2.5 [25]
CaO	<0.090	0.306	0.110	
MgO	0.038	0.363	0.350	
K_2O	1.140	0.975	1.970	
MnO_2	0.028	0.026	0.030	
Na_2O	0.048	0.185	0.070	
TiO_2	0.004	1.380	0.390	
P_2O_5	0.009	0.049	<0.010	
LoI [wt %]	12.600	8.100	-	-

press, to yield bricks of 248x123x66 mm. The brick samples were dried and fired in a tunnel kiln at 1350°C for 7-8 hours and slowly cooled during exit of the furnace. The sintered bricks had an average dimension of 232x116x62 mm. Out of them, cylindrical test-pieces of diameter approximately 50 mm and height 50 mm were cut and used for determining apparent porosity, bulk density, cold crushing strength, permanent linear change in dimension, water absorption, refractoriness under load, and thermal shock resistance.

Characterization of fired bricks. The chemical composition of a sintered brick sample was determined by wet ICP-AES of ignited sample brick powder at Lafarge Svenska Höganäs AB, Sweden [14].

The extent of vitrification was determined in some physical properties such as water absorption, linear shrinkage, apparent porosity and bulk density. Linear shrinkage of the bricks was determined by taking the ratio of the sintered brick dimensions and those of the green sample. The results are shown in **Table 2**.

Water absorption, apparent porosity, and bulk density were measured using the standard water immersion method following the PRE/R 9, 78, p.1 [15] procedure. Three cylindrical samples were used. They were first dried in an oven at 110°C. Then, they were weighed and the dry individual masses were recorded as m_1. The dried and cooled test pieces were then placed in an airtight vessel. After sealing the vessel, it was evacuated until a constant pressure of 25 mbar was attained. Water was introduced into the vessel to submerge all the samples. This environment was maintained for 30 minutes after which the vacuum was released and the samples were removed from the water. Each of the test pieces was weighed while completely immersed in water on a hydrostatic balance and its mass was recorded as m_2. The test pieces were removed one by one from the water and sponged to remove droplets and the surface film of water. Immediately each test piece was weighed in air and its mass recorded as m_3. The properties of the test pieces were determined as average values from the following standard equations:

$$Bulk\ density = \frac{m_1}{m_3 - m_2} \cdot \rho \quad (1)$$

$$Apparent\ porosity = \frac{m_3 - m_1}{m_3 - m_2} \cdot 100 \quad (2)$$

$$Water\ absorption = \frac{m_3 - m_1}{m_1} \cdot 100 \quad (3)$$

Where ρ = density of water = 997 kgm^{-3} at 25°C.

Determination of the cold compressive strength of the sintered samples was done according to PRE/R 14-1, 90, p.1 [16]. Three cylindrical test-pieces from three different sintered sample bricks were tested. Each test piece was subjected to a steadily increasing compressive pressure at a rate of about 1 Nmm^{-2}s^{-1} until it failed. The maximum load was recorded and the compressive strength was calculated from the ratio of collapsing load and the cross-sectional area of each test piece. The compressive strength of the sample was computed as the average strength of the three test pieces.

Determination of permanent linear change in dimension was carried out in conformance with PRE/R 19, 78, p. 1 [17]. Three cylinder test pieces from different sintered bricks were used. Before heating, four points were marked along the length of each test-piece. Diameter at each mark was measured and recorded. The test-pieces were heated in an electric furnace from room temperature to 1200°C at a rate of 10°Cmin^{-1} and between 1200-1350°C at 5°C/min and between 1350 and 1400°C at 2°Cmin^{-1} and held at 1400°C for 5 hours. On cooling to ambient conditions, the diameters of each test piece were measured at the previously marked points. The change in dimension was determined for each test-piece and an average value was recorded.

Thermal conductivity of the sample bricks was determined by the hot wire method and following the PRE/R 32, 78, p.1 [18] procedure for testing dense refractories. A test assembly consisting of two flatly-ground bricks (235x115x61 mm) was used. It is recommended to use a full-sized shape when evaluating thermal conductivities of materials with a coarse microstructure, such as refractories [19]. Two straight grooves for the measuring crosspiece and a V-groove for the reference thermocouple were machined in the upper contact face of the bottom piece. The cemented test assembly was heated in a Netsch TCT-426 instrument in atmospheric environment. The heating was done in steps of 500°C, 750°C, 1000°C and 1250°C. Three measurements were made for each step and the average values of thermal conductivity determined.

Thermal shock resistance was carried out by repeatedly heating three cylindrical samples to 950°C in an atmospheric environment and quenching them in running cold water at about 20°C, following PRE/R 5.1, 78, p.1 [20]. The extent of cracking was observed at each cycle and the experiment ended when too many cracks were developed in the test piece.

Determination of refractoriness-under-load was carried out in conformance of PRE/R 4, 78, p.1 [21]. A cylindrical test-piece with an axial hole of 12.5 mm was used. The test

Table 2. Properties of the prepared sample bricks in comparison with commercial types.

Property	Achieved value	Commercial types
Bulk density [kg/m^3]	1938	1900-2000 [4,23,25]
Apparent porosity [%]	24.6	22-26 [4,25]
Water absorption [%]	12.6	
Shrinkage [%] • linear • volumetric	 6.1 17.0	
Cold crushing strength [MPa]	44.0±2.2	>20 [4]
Thermal shock resistance [cycles]	10±1	>10 [4,25]
Refractoriness under 0.2 MPa load [°C]	T_{05}:1290 T_1: 1350 T_2: 1380 T_5: 1420	≈1230 [23]
Permanent linear change (1400°C, 5h), [%]	-1.9±0.17	±3 [29]
Alkali resistance [cm^2]	1.2	1.7

assembly was comprised of a coaxial loading device (applying a constant co-axial pressure of 0.2 MPa), a supporting column and the test piece supported between two alumina hollow discs. The assembly was put in a bell furnace and heated at 5°C/min. The deformation of the test piece was recorded as the temperature increased. The temperatures corresponding to four pre- defined deformations of the test piece were determined from the plot of percentage change in height versus temperature.

The microstructure of the fired samples was studied by scanning a carbon coated sample with a Field Electron Gun Scanning Electron Microscope (FEG-SEM), LEO 1530 with a GEMINI column. A cube of about 1 cm was cut from the sintered brick and polished well. In order to reveal the mullite crystals, it was etched for 30s in concentrated hydrofloride acid. The cube was then coated with carbon to avoid the charging effect during scanning. In addition, a thin section was also taken from a sintered brick sample, glued on a piece of glass, ground and polished properly. It was then observed in a light optical microscope under polarized light (see **Figure 1 and 2**).

For phase characterization, a randomly oriented powdermount of a crushed sintered brick was scanned over the range 12 to 60° 2θ using a Philips X-ray Diffractometer, PW 1130/90, with Ni-filtered K_α Cu-radiation, operated at 40 kV and 30 mA. An energy dispersive detector of type Kevex was used. The collimator and receiving slits were set to 1 and 0.1°, respectively. The X-ray scans are shown in **Figure 3 and 4**. The observed peaks were correlated with the corresponding phase compositions in the equipment database.

To ascertain the corrosive resistance of the sintered bricks, an alkali test was carried out using the crucible method. A sintered brick was selected from the batch and split into two halves along its length. A hole, 50 mm diameter and a depth of 40 mm, was drilled in the middle of one of the divided brick pieces. The prepared brick sample was dried in an oven at 110°C. The hole in the brick was then filled with 50 g K_2CO_3 and covered with a cemented lid. The test sample was then put in an electric lab furnace ramping at 100°C/h until it reach 1100°C and was then held there for 5h. After completed holding time, the furnace was allowed to cool down (naturally) to room temperature. The sample was taken out, dissected into two halves and the extent of the alkali attack was determined by measuring the area of the affected cross section area.

Results and Discussion

Chemical composition. For the production of fireclay refractories from naturally occurring materials, it is essential that the chemical composition of the mixture should be within 25-45 wt% alumina and that the total amount of fluxes should be below 5% [3,4,22-25]. As seen from **Table 1**, the present sample bricks are composed of 30.6 wt% alumina, 64.7 wt% silica and 3.8 wt% fluxes. Thus, they readily fulfill the recommendations and it is especially interesting to note the low amounts of Fe_2O_3 and TiO_2, 0.88 wt% and 0.39 wt%, respectively. These values are substantially lower than the values of 3% and 2.5% which are normally accepted. Actually, it is tempting to lower the amount of fluxes further in order to limit the reduction in liquidus temperature from the binary SiO_2-Al_2O_3 system. Although the liquidus temperature is an important indicator of the thermal, chemical and mechanical properties at high temperatures, fluxes also promote glass formation and facilitate the formation and crystallization of principle phases during sintering. Thus, a small amount is beneficial in the production process.

Microstructure and phase analysis. On firing kaolinitic minerals, kaolin transforms to metakaolinite (400-500°C), metakaolinite transforms to a spinel ($SiAl_2O_4$) and amorphous silica (SiO_2) between 950-1100°C and finally to mullite ($3Al_2O_3{\cdot}2SiO_2$), quartz (SiO_2) and a glass phase. The SEM micrographs of a chemically etched sample brick, **Figure 1**, confirms that the microstructure consists of a network of mullite needles evenly distributed and embedded in a glassy phase. The abundance of well crystalline mullite confirms a good sintering and promotes a high cold crushing strength and high corrosion resistance, as will be discussed later.

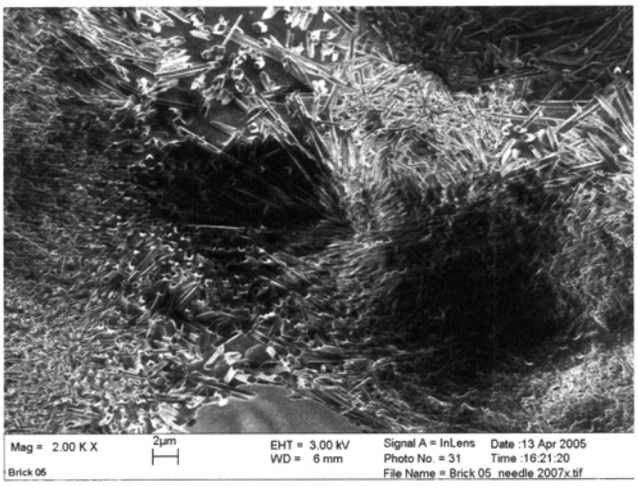

Figure 1. SEM image of a sintered brick, polished and etched in conc. HF for 30s.

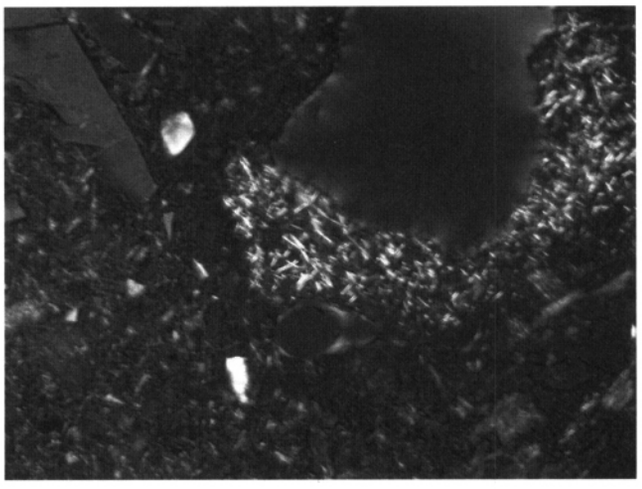

Figure 2. Thin transparent section of a sintered brick in polarized light.

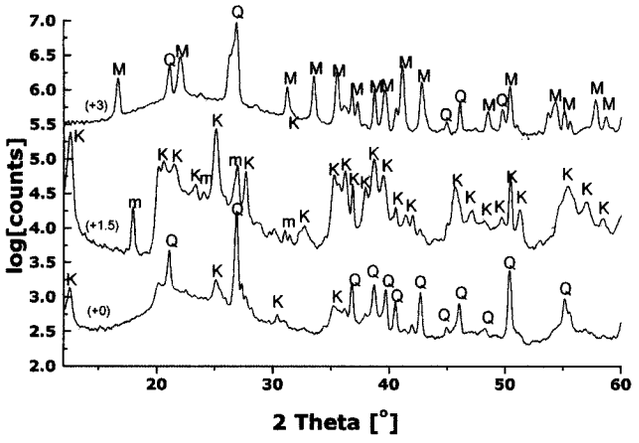

Figure 3. XRD scans of raw powders of the raw materials and a crushed sintered brick powder. Mukono ball clay (+0), Mutaka kaolin (+1.5), sintered brick (+3). Numbers in parenthesis show the vertical displacement of the curves. M, Q, K and m represent mullite, quartz, kaolinite and muscovite respectively.

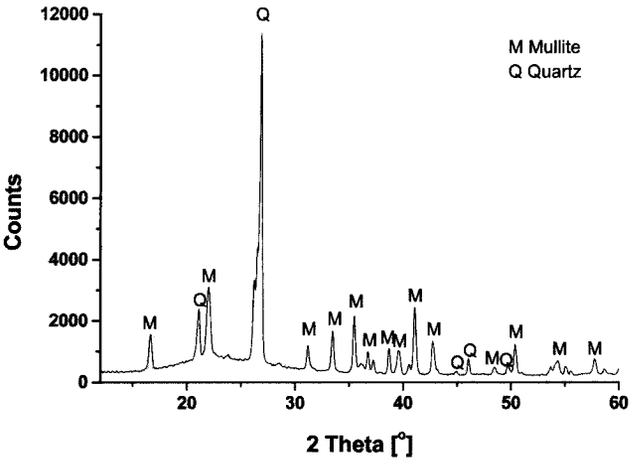

Figure 4. XRD scan of a powder prepared from a sintered brick.

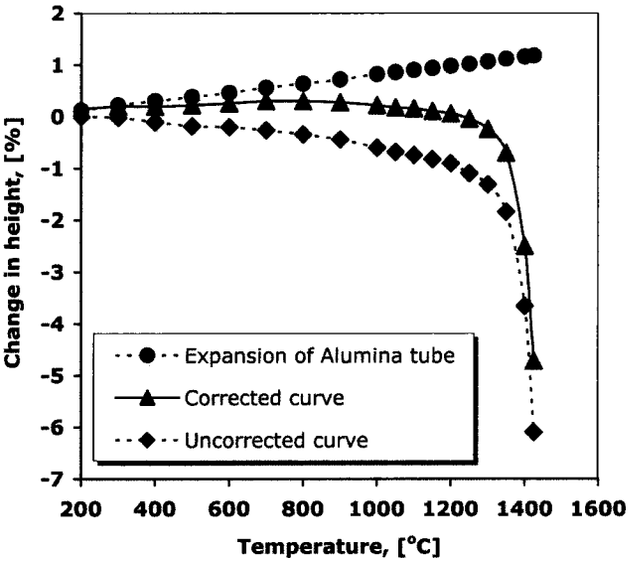

Figure 5. Refractoriness under a constant load of 0.2 MPa and a heating rate of 5°Cmin^{-1}.

A thin section observed under polarized light, **Figure 2**, is in agreement with the SEM findings, showing a mullitized sintered brick. The mullite grains, white needle-like crystals around the middle pore are embedded in the glassy phase. The blue and yellow structures are quartz while brown structures represent grog crystals.

The XRD scans of the raw materials used to formulate the brick and of the final brick are shown in Figure 3 and 4. In **Figure 3**, the logarithmic values of the intensity counts are given in order to suppress the peak heights. For easy comparison, the curves are vertically displaced. As seen, the kaolinite and muscovite present in the raw materials are replaced by mullite and quartz in the sintered brick, thus confirming the SEM findings. In **Figure 4**, the XRD scan of the sintered brick is shown. As seen, a glass phase is indicated by the wide bump between 15 and 30° 2θ.

Physical properties. The bulk density, apparent porosity, water absorption and shrinkage of the end brick are tabulated in Table 2. The sintering parameters, i.e. high density and low porosity are improved by high firing temperature. It is apparent that the sample bricks had gone through a great extent of sintering at 1350°C with a corresponding volumetric shrinkage of about 17%. As seen, the bulk density is relatively low and the apparent porosity is relatively high, which is a consistent finding. The high porosity is a result of the combined effects of shrinkage during sintering and loss on ignition from the added 20% uncalcined binder material. The former lowering the porosity while the latter increasing it. Naturally, the binder cannot be calcined because it would then lose its ability to bind the grog and provide sufficient green strength to the formed brick. Since water absorption is about half of the apparent porosity, it indicates that many pores are closed.

Mechanical properties. The average cold crushing strength of the brick is 44.0 MPa. Considering the low density and high porosity, it would be expected that the cold crushing strength would be low. However, it is falling well above the strength range of similar commercial types which is very encouraging. As reported earlier in literature [26-32], formation of mullite during sintering promotes high strength. As was shown earlier, SEM and XRD investigations confirm a rich formation of this important phase.

Thermal properties. The thermal conductivities of the bricks at nominal temperatures from 500 to 1250°C are given in **Table 3** and shown in **Figure 6**. As seen, conductivity increases linearly with temperature which is typical to dense bricks, like the present one. In a dense brick heat conduction through the brick material is more important than radiation. On the other hand, in a light brick, like insulating bricks, the heat conduction by radiation is much more important. Since the latter follows the T^4-law, one may conclude that it is of less importance in the present brick.

The thermal shock averages 10 cycles, which is just reaching the lower limit of similar plastically pressed fireclay refractories. Thermal shock is one of the most important properties that characterize the behaviour of a refractory during sudden temperature shock. This frequently hap-

pens during intermittent operation of furnaces and can lead to disintegration or spalling of the brick structure. The relatively poor thermal shock resistance of the present brick justifies its use in environments of more stable temperatures.

Refractoriness under load is a vital property of refractories since the time of service of a refractory is determined by its deformation under load at high temperature, finally leading to failure. The test serves to evaluate the softening behaviour of fired refractory bricks at rising temperature and constant stress conditions. Results of the refractoriness under 0.2 MPa load are summarized in the three curves shown in Figure 5. The effective refractoriness under load curve (corrected) is obtained by adding the brick subsidence curve (uncorrected) and the corresponding alumina tube expansion curve. The corrected curve shows that on heating from 200-800°C the brick slightly expands. It starts to shrink gradually between 900-1300°C after which drastic subsidence starts. Deformations corresponding to 0.5%, 1.0%, 2.0% and 5.0% of the initial height of the test piece can be obtained from the corrected curve and are given in Table 2. $T_{0.5}$ corresponds to the beginning of subsidence and T_5 corresponds to beginning of failure i.e. the brick cannot work above this temperature.

Refractories are complex ceramic structures composed of crystalline phases (mullite and quartz in fireclay), a glass phase, pores and cracks. At high temperatures the glass phase, binding the crystalline phases, becomes soft. At this point the crystalline phases start to slide against each other leading to creep. If the temperature is further increased, the viscosity is rapidly lowered and the creep rate rapidly increased, as indicated in **Figure 5**. As a result, the maximum operation temperature of the present brick must be limited to 1300°C.

As pointed out previously, the present brick has a high porosity value which actually falls in the upper region of comparable brick types. As the pores do not contribute to the loading capacity, it is very encouraging to note the $T_{0.5}$ is some 60°C higher than that of similar brick types. One may suggest that this good result is attributed to the relatively low amount of impurities in the raw materials.

Alkali resistance test. Impurities in refractory phases are known to reduce the corrosive resistance of refractories since they are rapidly attacked by corrosive liquids and gases, especially at high temperatures. Fireclay refractories are chemically acidic and react with alkaline substances. Results of the corrosion resistance test show that the affected area of the sample brick is 1.2 cm^2 as compared to 1.7 cm^2 of a similar commercial brick. This is attributed to the low impurity content (3.8%) and in particular the low Fe_2O_3 content (0.88%). In addition, the high mullite content achieved during sintering, results in a high corrosion resistance since this phase is known to enhance corrosion resistance [26, 27, 29].

Conclusions

The results of the technological properties of the prepared fireclay brick samples compare favourably with those of the parallel commercially produced bricks. The achieved properties are attributed to the right choice of powder mixes and a thorough thermal treatment leading to good sintering properties. The sintering process is promoted by a reasonable amount of fluxing oxides which contribute to formation of a glass phase that binds the mullite crystals. Consequently, these bricks can be used judiciously as general purpose bricks for reheating furnaces, rotary cement kilns, checkers, boilers, ladles, non-ferrous metal furnaces, waste incinerators and for other processing industry applications. In light of the foregoing investigations, the kaolin from Mutaka and ball clay from Mukono are the deposits recommended as viable and reliable supply of raw materials for the manufacture of fireclay refractory bricks.

Table 3. Thermal conductivity of the sintered bricks at various mean temperature.

Temperature [°C]	Thermal conductivity [$Wm^{-1}K^{-1}$]
500	1.22
750	1.49
1000	1.61
1250	1.82

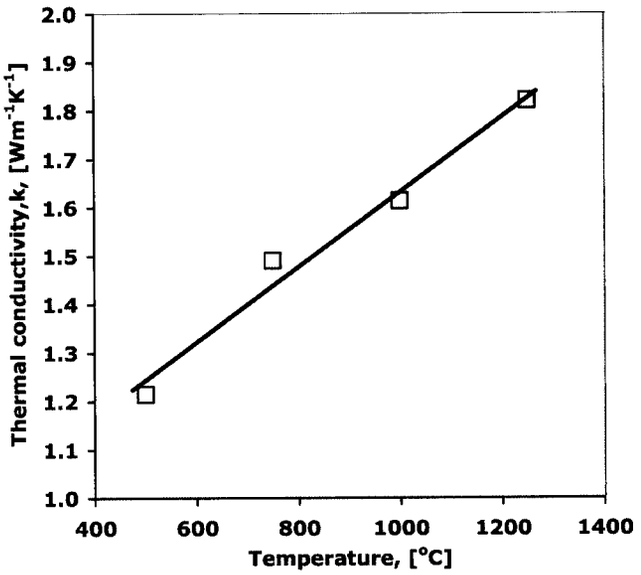

Figure 6. Thermal conductivity of a sintered brick.

Acknowledgements

The authors of this paper would like to appreciate the financial support from the Swedish Sida/SAREC-Makerere University Research Collaborative Programme in the Lake Victoria Region, for fully financing this work. They are also grateful to the following collaborating Institutions; Royal Institute of Technology (KTH), Sweden; Department of Geological Survey and mines, Entebbe, Uganda: Höganäs Bjuf Refractories AB, Bjuv, Sweden and the School of Graduate Studies, Makerere University, Kampala, Uganda.

(SJM 5831, originally submitted to Scandinavian Journal of Metallurgy, received on 13 May 2005, accepted in revised form on 6 July 2005)

Contact: John Baptist Kirabira, Department of Mechanical Engineering, Makerere University, P.O. Box 7062, Kampala, Uganda. Email: jbkirabira@tech.mak.ac.ug

References

[1] Carniglia S.C. and Barna G.L.: Handbook of Industrial Refractories Technology: Principles, types, properties and applications, Noyes Publications Westwood, New Jersey, USA, 1992, 6-23.

[2] Searle A.B.: Refractories for furnaces, kilns, retorts, etc., Cosby Lockwood & Sons, Ltd., London, 1964.

[3] Budnikov P.P.: The technology of ceramics and refractories, MIT Press, Cambridge, MA., 1964.

[4] Didier Refractory Techniques. Refractory materials and their properties, Didier-Werke AG, Wiesbaden, Germany, 18-38.

[5] Kirabira J.B., Jonsson S. and Byaruhanga J.K.: J. Australasian Cer. Soc., 40 (2004), No. 2, 12-19.

[6] Nyakairu G.W., Koeberl C. and Kurzweil H.: Geothermal Journal, 35 (2001), 245-256.

[7] Serry M.A., El-Kholi M.B., Elmaghraby M.S., Telle R.: Ceramics Int., 28 (2002), 575-583.

[8] Ghosh S., Mihir Das, Chakrabarti, S., and Ghatak, S.: Ceramics Int., 28 (2002), 393-400.

[9] Abadir M.F., Sallam E., Bakr I.M.: Ceramics Int., 28 (2002), 303-310.

[10] Kungurtsev V.N., Mironova L.V., Kochubeev Yu.N., Borisova Yu. A.: Refractories and Industrial Ceramics, 43 (2002), No. 1-2, 19-21.

[11] Mitchell D. and Vincent A.: Applied Clay Science 11 (1997), 311-327.

[12] Lugoye N.M.E.: A study of the properties of local materials for production of engineering refractories, Master of Science thesis. University of Dar es salaam Library, 1998.

[13] Kirabira J.B., Jonsson S., Byaruhanga J.K.: Powder characterization of high temperature ceramic raw materials in the Lake Victoria region. In press, Silicates Industriels.

[14] Larfage Svenska Höganäs AB, Bruksg. 37, Box 216, 236 23 Höganäs, Sweden.

[15] PRE/R 9, 78, p.1. Recommendations, 1990 for determination of density, apparent porosity and porosity of dense shaped refractory products.

[16] PRE/R 14-2, 90, p1. Recommendations 1990 for determination of cold crushing strength of dense shaped refractory products: PRE (Federation Européenne des Fabricants de Produits réfractaires) Refractory Materials, Recommendations, 1990, According to ISO/R 836. Zurich, Switzerland.

[17] PRE/R 19, 78, p.1. Recommendations 1990 for determination of the permanent change in dimensions under the action of heat of dense shaped refractory products.

[18] PRE/R 32, 78, p.1. Recommendations 1990 for determination of thermal conductivity up to 1500°C for values of $\lambda \leq 1.5 Wm^{-1}K^{-1}$ by the hot wire method.

[19] Akiyoshi M.M., Da Silva A.P. Da Silva M.G., Pandolfelli V.C.: Am. Cer. Soc. Bull., 81 (2002), No. 3, 39-43.

[20] PRE/R 5.1, 78, p.1. Recommendations 1990 for determination of resistance to thermal shock.

[21] PRE/R 4, 78, p.1. Recommendations 1990 for determination of refractoriness-under-load with rising temperature.

[22] Gilchrist J.D.: Fuels, Furnaces and Refractories, Pergamon Press, UK, 1997.

[23] Routschka G. (Ed.): Pocket manual - Refractory Materials: Basics, Structures and Properties. 2nd Edition, Vulkan-Verlag Essen, 2004, 51-83

[24] Shaw K.: Refractories and their uses, Applied Science Publishers, London, 1972, 81-97.

[25] Refractories Handbook. The Technical Association of Refractories, Japan, 1998.

[26] Aksel C.: Materials Letters, 57 (2002), 708-714.

[27] Schneider H., Okada K., Pask J.A.: Mullite and mullite ceramics, John Wiley and Sons, 1994, 83-103.

[28] Bakunov V.S. and Belyakov A.V.: Refractories and Industrial Ceramics, 41 (2000), No. 9-10, 349-355.

[29] Chesters J.H.: Refractories: Production and properties, Iron and Steel Institute, London, 1973.

[30] Obadia S. and Broussaud D.: Sci. Ceram., 14 (1988), 431-436.

[31] Johnson S.M. and Pask J.A.: Am. Ceram. Soc. Bull., 61 (1982), No. 8, 838-842.

[32] Sainz M.A., Serrano F.J., Amigo J.M., Bastida J., Caballero A.: J. Eur. Ceram. Soc., 20 (2000), 403-412.